Entanglement of arbitrary superpositions of modes within two-dimensional orbital angular momentum state spaces

B. Jack,[1] A. M. Yao,[2] J. Leach,[1] J. Romero,[1,2] S. Franke-Arnold,[1] D. G. Ireland,[1] S. M. Barnett,[2] and M. J. Padgett[1]
[1]*Department of Physics and Astronomy, Scottish Universities Physics Alliance, University of Glasgow, Glasgow G12 8QQ, United Kingdom*
[2]*Department of Physics, Scottish Universities Physics Alliance, University of Strathclyde, Glasgow G4 0NG, United Kingdom*
(Received 27 October 2009; published 30 April 2010)

We use spatial light modulators (SLMs) to measure correlations between arbitrary superpositions of orbital angular momentum (OAM) states generated by spontaneous parametric down-conversion. Our technique allows us to fully access a two-dimensional OAM subspace described by a Bloch sphere, within the higher-dimensional OAM Hilbert space. We quantify the entanglement through violations of a Bell-type inequality for pairs of modal superpositions that lie on equatorial, polar, and arbitrary great circles of the Bloch sphere. Our work shows that SLMs can be used to measure arbitrary spatial states with a fidelity sufficient for appropriate quantum information processing systems.

DOI: 10.1103/PhysRevA.81.043844 PACS number(s): 42.50.Tx, 03.65.Ud, 42.40.Eq

I. INTRODUCTION

The violation of a Bell-type inequality is the hallmark of quantum entanglement. In the past couple of decades, bipartite quantum entanglement has been of interest both within the context of quantum information theory [1] and quantum computing [2,3] and for applications such as entangled cryptographic systems [4] and quantum imaging [5–7]. Initially demonstrated for polarization [8–11], entanglement has also been shown between conjugate variables such as time and energy [12,13], position and momentum [14], and also multiple variables simultaneously (known as hyperentanglement) [15].

Entanglement has also been demonstrated between spatial modes carrying orbital angular momentum (OAM) and has been used for quantum information protocols [16–23]. These helically phased modes have an azimuthal phase dependence $e^{i\ell\varphi}$ and carry an OAM of $\ell\hbar$ per photon [24]. The spatial modes of light are defined within an infinite-dimensional, discrete Hilbert space and there is considerable potential for their use within applied quantum systems [25,26]. For example, a simple displacement of a spiral phased hologram with respect to the beam axis introduces additional modes in an OAM superposition, thereby expanding the dimensionality of the Hilbert space [18,19]. In our work we use spatial light modulators (SLMs) to restrict ourselves to a two-dimensional (2D) OAM subspace, selected from the complete state space. Within this subspace, by using measurement holograms that control both the phase and the intensity of the light we can measure any complex superposition of ℓ and $-\ell$ states, each represented as a point on a sphere [27], analogous to the Bloch sphere [2] as shown in Fig. 1.

In this paper we demonstrate that photon pairs generated by parametric down-conversion are entangled in arbitrary superpositions of OAM modes, and that the use of SLMs allow us to access the entire 2D state space of the OAM. For this we measure the correlations between pairs of modal superpositions, each described by arbitrary positions on the Bloch sphere. This is only possible through manipulation by the SLM of both the phase and the intensity of the measured state. From these correlations we violate a Bell inequality [28] for superpositions that are represented by equatorial, polar, and arbitrary great circles around the Bloch sphere, demonstrating that these superpositions remain highly entangled.

II. THEORY

Each point on the Bloch sphere (Fig. 1) describes a different pure state and its antipode represents the orthogonal state. In general, a state $|\mathbf{a}\rangle$ can be written as

$$|\mathbf{a}\rangle = \cos\left(\frac{\theta_a}{2}\right)|\ell\rangle + e^{i\phi_a}\sin\left(\frac{\theta_a}{2}\right)|-\ell\rangle, \tag{1}$$

where $\mathbf{a} = (\sin(\theta_a)\cos(\phi_a), \sin(\theta_a)\sin(\phi_a), \cos(\theta_a))$ is a vector with latitude $0 \leqslant \theta_a \leqslant \pi$ and longitude $0 \leqslant \phi_a < 2\pi$, as shown in Fig. 1. The longitudinal position ϕ on the sphere is the phase between the two superposed modes and relates to the orientation of the mode superposition. It is related to the azimuthal phase of the mode via $\phi = 2\ell\varphi$, where φ relates to the orientation of the mode (i.e., it is the azimuthal coordinate in real space for a Laguerre-Gauss mode [24]) For example, the orientation angle between the two orthogonal modes of, say, the HG_{20} mode is $\pi/4$, while the phase between the superposed Laguerre-Gauss modes (± 2) is π. Hence, the states $|\ell\rangle, |-\ell\rangle$ correspond to the poles of the sphere ($\theta_a = 0,\pi$), respectively, while equally weighted superpositions of $|\ell\rangle$ and $|-\ell\rangle$ correspond to points around the equator ($\theta_a = \pi/2$), with the equatorial position determined by the phase term ϕ_a between the two states.

Photons produced by spontaneous parametric down-conversion conserve OAM under the conditions of approximately collinear phase matching [16] and for small non-collinear opening angles where the paraxial approximation can still be applied [29]. Thus, for an $\ell = 0$ pump, if a signal photon is measured in state $|\ell\rangle$ then the idler must be in the state $|-\ell\rangle$, with an associated probability amplitude c_ℓ where $c_\ell = c_{-\ell}$ because the process is symmetric.

For a pump with $\ell = 0$, the two-photon field produced can be written as

$$|\psi\rangle = \sum_{\ell=-\infty}^{\ell=\infty} c_\ell |-\ell\rangle_A |\ell\rangle_B, \tag{2}$$

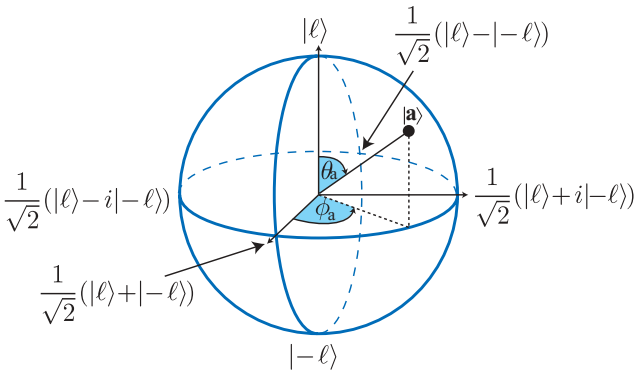

FIG. 1. (Color online) Bloch sphere equivalent for $\pm\ell$ OAM states. The pure state $|\mathbf{a}\rangle$ is defined by its latitude $(0 \leqslant \theta_a \leqslant \pi)$ and longitude $(0 \leqslant \phi_a < 2\pi)$ on the sphere. The poles $(\theta_a = 0,\pi)$ represent the states $|\ell\rangle,|-\ell\rangle$, respectively, while around the equator $(\theta_a = \pi/2)$ are the equally weighted superpositions of $|\ell\rangle$ and $|-\ell\rangle$.

where A and B denote the photons measured with SLMs A and B, respectively, and $|\ell\rangle$ denotes a one-photon state with OAM $\ell\hbar$.

We restrict ourselves to a two-dimensional Hilbert space by making measurements that are sensitive only to the photons spontaneously prepared in this space. The two-photon state, for the 2D subspace, can be written in the normalized form

$$|\psi\rangle = \frac{1}{\sqrt{2}}(|\ell\rangle_A|-\ell\rangle_B + |-\ell\rangle_A|\ell\rangle_B). \tag{3}$$

Each single-photon measurement outcome corresponds to projection onto a state of the form of Eq. (1). The measurement states for the two photons can be oriented in different directions θ_a,ϕ_a and θ_b,ϕ_b, represented by the Bloch vectors $\mathbf{a}$ and $\mathbf{b}$, respectively. The coincidence rate $C(\mathbf{a},\mathbf{b})$ for detecting one photon in state $\mathbf{a}$ and the other in $\mathbf{b}$ is, for the entangled state (3),

$$\begin{aligned} C(\mathbf{a},\mathbf{b}) &\propto |\langle\mathbf{a}|\langle\mathbf{b}|\psi\rangle|^2 \\ &= \tfrac{1}{4}[1 - \cos(\theta_a)\cos(\theta_b) \\ &\quad + \sin(\theta_a)\sin(\theta_b)\cos(\phi_a - \phi_b)]. \end{aligned} \tag{4}$$

Therefore, we predict *maximum* coincidence for $\theta_b = \pi - \theta_a$ and $\phi_b = \phi_a$, corresponding to states with the same longitude but reflected about the equator, and *minimum* coincidence for $\theta_b = \theta_a$ and $\phi_b = \phi_a - \pi$, corresponding to states with the same latitude but reflected about the vertical axis, as shown in Fig. 2.

An experimentally appropriate Bell-type inequality is the Clauser-Horne-Shimony-Holt (CHSH) inequality [8,31,32], $-2 \leqslant S \leqslant 2$, where

$$S = E(\mathbf{a},\mathbf{b}) - E(\mathbf{a},\mathbf{b}') + E(\mathbf{a}',\mathbf{b}) + E(\mathbf{a}',\mathbf{b}'). \tag{5}$$

Here $\mathbf{a},\mathbf{a}'$ and $\mathbf{b},\mathbf{b}'$ correspond to two different measurement states, selected by the appropriate holograms on SLMs A and B, respectively, and

$$E(\mathbf{a},\mathbf{b}) = \frac{C(\mathbf{a},\mathbf{b}) + C(-\mathbf{a},-\mathbf{b}) - C(\mathbf{a},-\mathbf{b}) - C(-\mathbf{a},\mathbf{b})}{C(\mathbf{a},\mathbf{b}) + C(-\mathbf{a},-\mathbf{b}) + C(\mathbf{a},-\mathbf{b}) + C(-\mathbf{a},\mathbf{b})}, \tag{6}$$

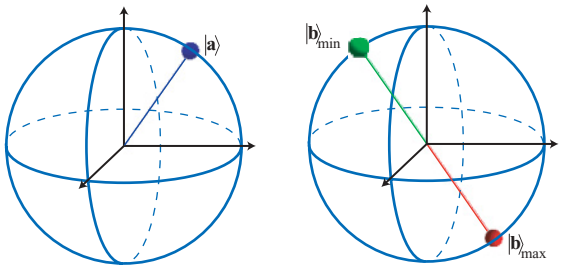

FIG. 2. (Color online) For measurements of state $|\mathbf{a}\rangle$ (left), the state measurement of the other photon $|\mathbf{b}\rangle$ will yield maximum coincidence when the state has the same longitude and is reflected about the equator and minimum coincidence when the state has the same latitude and is reflected about the vertical axis (right).

where $C(\mathbf{a},\mathbf{b})$ is the observed coincidence count rate, which is predicted to be of the form of Eq. (4).

In previous work we demonstrated the violation of a Bell inequality by measuring the correlations between equally weighted superpositions of two pure OAM states, $|\pm\ell\rangle$, of differing relative phase [22]. Measurement of these states, which lie on the equator of the Bloch sphere, were made using SLMs acting as holograms to define ℓ-fold rotationally symmetric sector states. The measurements using these phase-only sector states in order to violate a Bell-type inequality was appropriate in these cases due to the limited spiral bandwidth and negligible amplitude of higher-order modes. Similarly we have reported the full density matrix reconstructions for $\pm\ell$ subspaces [30], which require additional measurements of the pure OAM states (which lie at the poles of the Bloch sphere). Although the density matrices are a full predictor of the anticipated correlation of all possible measurements, they are not a test of the ability to make arbitrary measurements, and they are not a test of local hidden-variable theories. These measurements are analogous to measuring the pure linear (equatorial) and circular (polar) states of polarization. In this present work, our measurements are equivalent to measuring states of elliptical polarization.

In this work, therefore, the design of our SLM holograms is necessarily more sophisticated than that in our earlier work and incorporates a spatially dependent blazing function to create an intensity mask that is superimposed on the phase mask. This is the same approach that we used previously to create complicated superpositions of modes, in the classical domain, for the generation of optical vortex knots [33]. The phase distribution of the hologram, $\Phi(x,y)_{\text{holo}}$, can be expressed within the range from $-\pi$ to π as

$$\begin{aligned} &\Phi(x,y)_{\text{holo}} \\ &= \{[\Phi(x,y)_{\text{beam}} + \Phi(x,y)_{\text{grating}}]\}_{\text{mod}2\pi}\,\text{sinc}^2\{[1 - I(x,y)\pi]\}, \end{aligned} \tag{7}$$

where $\Phi(x,y)_{\text{beam}}$ is the phase distribution of the beam, $\Phi(x,y)_{\text{grating}}$ is the phase distribution of a blazed diffraction grating, and $I(x,y)$ is the desired intensity. The sinc^2 term accounts for the mapping of the phase depth to the diffraction efficiency of the spatially dependent blazing function.

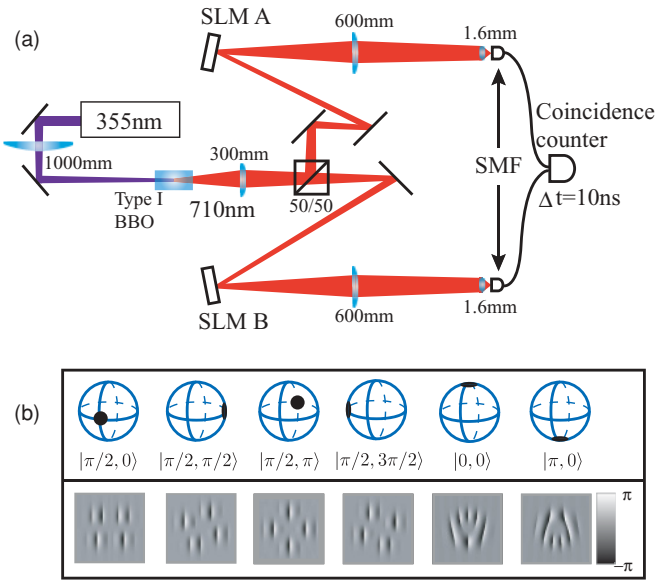

FIG. 3. (Color online) (a) Experimental setup. The down-converted light from the crystal is imaged onto the SLMs, and then reimaged at the plane of the single-mode fibers, where the detection and coincidence measurement takes place. (b) Typical phase masks—with appropriate intensity blazing—as would be displayed on an SLM. Shown are the two OAM eigenstates and four equally weighted superposition states (Laguerre-Gauss and Hermite-Gauss, respectively).

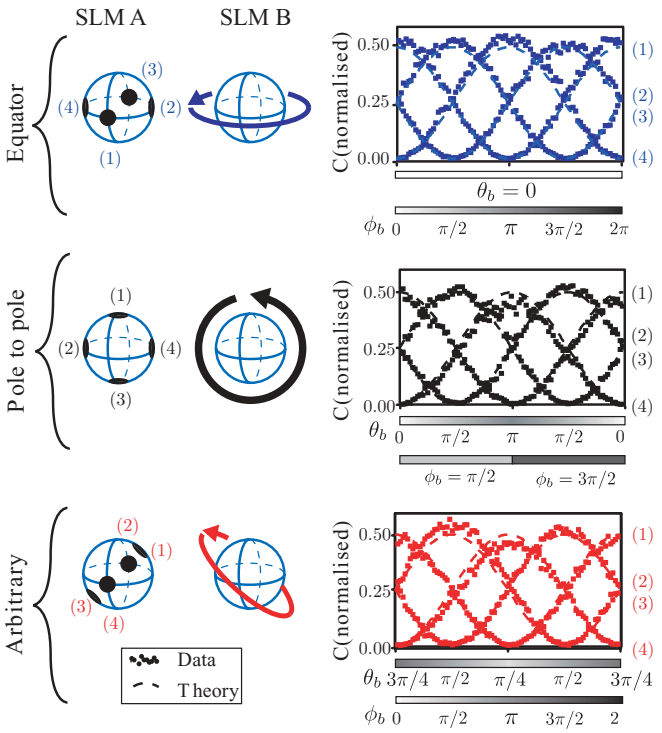

FIG. 4. (Color online) Bell curves for three different great circles around the equator, poles, and an arbitrarily chosen great circle. Each curve corresponds to coincidence measurements between a state on a great circle around one Bloch sphere (right) and one of four different static states (left), shown as points on the spheres. The sinusoidal fringes are indicative of quantum correlations within a purely two-dimensional subspace, and each example shown violates a Bell inequality.

III. EXPERIMENT

Our experimental setup (see Fig. 3) uses a 150-mW pump laser of wavelength 355 nm incident on a 3-mm-long β-barium borate crystal tuned for type I, collinear down-conversion. The 710-nm down-converted photons are separated by a 50/50 beam splitter and imaged onto SLMs (Hamamatsu liquid crystal on silicon) and then reimaged onto the facets of single-mode fibers which are coupled to two spatially separated single-photon counting modules (PerkinElmer). The magnifications are set so that the 5-μm-diam facets of the fibers form 2-mm images at the SLMs and 300-μm overlapping images at the crystal, which are smaller than the 500-μm beam waist of the pump. The single-channel Transistor-transistor logic (TTL) outputs of the counting modules are fed into a coincidence counter (Ortec). This allows us to measure both the single-channel and coincidence count rates as a function of the holograms displayed on SLMs A and B. Example forms of the measurement holograms are shown in Fig. 3(b).

IV. RESULTS

Our results, for the $\ell = \pm 2$ subspace, are shown in Fig. 4. In each case we plot the coincidence rate as one of the superpositions is scanned around a great circle of the Bloch sphere, while maintaining the other superposition at one of four equally spaced states, represented by the black dots. In Fig. 4, the measured states are positioned on the equator (as in our earlier work), from pole to pole and around an arbitrarily chosen great circle. As expected from Eq. (4), we observe sinusoidal fringes in the coincidence rate, characteristic of entanglement in two dimensions. In each case our results show a violation of a Bell-like inequality. We find the values of S to be 2.62 ± 0.06, 2.56 ± 0.05, and 2.59 ± 0.05 for the equatorial, polar, and arbitrary great circles in Fig. 4, respectively—clearly violating the constraints of a local, realistic hidden-variable theory.

A demonstration of the importance of modulating both the phase and the intensity of the holograms is shown in Fig. 5. Here the correlations are measured in a great circle around the poles again, but with holograms which represent only the phase of the desired state. In this case, it is clear that the measured variation in coincidence is not sinusoidal, and, hence, the phase-only holograms are inadequate for restricting the measurement space to two dimensions. It would be inappropriate to apply the CHSH inequality to these results, as the number of participating modes is no longer equal to 2.

In our method, we are not restricted to only measuring correlation between modes corresponding to great circles around the sphere. We are able to make coincidence measurements between *any* two superpositions of modes described by points $\mathbf{a}(\theta_a,\phi_a)$ and $\mathbf{b}(\theta_b,\phi_b)$, giving us access to the entire 2D state space (the entire surface of the Bloch sphere). We demonstrate this by choosing one particular point, $\mathbf{a}$, and varying $\mathbf{b}$ over the full range of possible values ($\theta_b = [0,\pi]; \phi_b = [0,2\pi]$). We can then map out a sphere of coincidence rate between the static state in arm A, with respect to the full

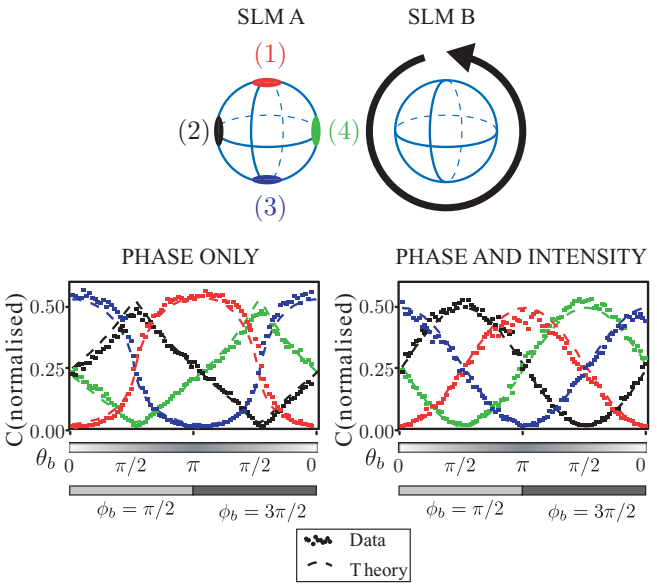

FIG. 5. (Color online) The necessary measurement of both the phase and the intensity of the modes. Pole-to-pole measurements (of the same type as in Fig. 4) are shown, but with only representations of the phase of the desired mode displayed on the SLM (left). The coincidence for the phase and intensity measurement (from Fig. 4) is shown for illustration (right). There is a clear difference between the form of the curves in each case, indicating that the number of modes selected in each case is different.

range of states measured in arm B. Our results are shown in Fig. 6(a) for reference holograms at a point on the equator ($\theta_a = \pi/2, \phi_a = 0$) and in Fig. 6(b) for reference holograms at a pole ($\theta_a = 0, \phi_a = 0$). As expected, we find that the coincidence rate varies sinusoidally in a great circle around the sphere with maximum counts when $\theta_b = \pi - \theta_a$ and $\phi_b = \phi_a$ and with minimum counts when $\theta_b = \theta_a$ and $\phi_b = \phi_a - \pi$.

V. CONCLUSIONS

In this paper we have demonstrated the use of SLMs to make precise measurements of arbitrary (but well-defined) superpositions of OAM states within a two-dimensional OAM subspace. This allows us to investigate the entanglement between spatial modes of photon pairs created in a spontaneous parametric down-conversion process. From precise control of

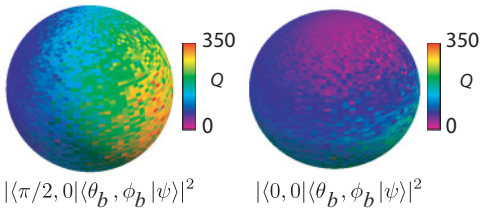

FIG. 6. (Color online) Two spheres in coincidence, shown with the same projection as Fig. 1. The scale shows the quantum contrast $Q = \frac{C}{S_1 S_2 \Delta t}$, where C is the measured coincidence rate, S_1, S_2 are the single count rates for each detector, and Δt is the gate time of our coincidence electronics.

holograms to shape both the phase and the intensity of the light, we can map out the coincidence rate between photon pairs over the entirety of a two-dimensional subspace within the higher-dimensional OAM Hilbert space. We then use these results to confirm the quantum nature of the entanglement, and to ensure the dimensionality of the state space is exactly equal to 2, by violating a Bell-type inequality between modal superpositions represented by equatorial, polar, and arbitrary great circles on the Bloch sphere. We note that the data required to do this are similar to that required to examine the Leggett-type inequalities [34–36]. It is possible that our system may permit a thorough exploration of the violation of these for OAM entangled states.

In conclusion, any applications that require the use and manipulation of complex OAM states may find this method and representation of states to be of practical value. Our work shows, moreover, that SLMs can be used to measure arbitrary spatial states with a fidelity sufficient for appropriate quantum information processing systems.

ACKNOWLEDGMENTS

This work is supported by the United Kingdom Engineering and Physical Sciences Research Council. SFA is a Research Councils UK Research Fellow. SMB and MJP thank the Royal Society and the Wolfson Foundation. We acknowledge the financial support of the Future and Emerging Technologies (FET) program within the Seventh Framework Programme for Research of the European Commission, under the FET Open Grant Agreement HIDEAS No. FP7-ICT-221906. We would like to thank Hamamatsu for their support of this work.

[1] M. B. Plenio and S. Virmani, Quantum Inf. Comput. **7**, 1 (2007).
[2] M. Neilsen and I. L. Chuang, *Quantum Computation and Quantum Information* (Cambridge University, Cambridge, England, 2000).
[3] S. M. Barnett, *Quantum Information* (Oxford University, New York, 2009).
[4] R. Ursin *et al.*, Nature Phys. **3**, 481 (2007).
[5] M. D'Angelo, Y.-H. Kim, S. P. Kulik, and Y. Shih, Phys. Rev. Lett. **92**, 233601 (2004).
[6] R. S. Bennink, S. J. Bentley, R. W. Boyd, and J. C. Howell, Phys. Rev. Lett. **92**, 033601 (2004).
[7] T. B. Pittman, Y. H. Shih, D. V. Strekalov, and A. V. Sergienko, Phys. Rev. A **52**, R3429 (1995).
[8] S. J. Freedman and J. F. Clauser, Phys. Rev. Lett. **28**, 938 (1972).
[9] A. Aspect, P. Grangier, and G. Roger, Phys. Rev. Lett. **47**, 460 (1981).
[10] A. Aspect, P. Grangier, and G. Roger, Phys. Rev. Lett. **49**, 91 (1982).
[11] W. Perrie, A. J. Duncan, H. J. Beyer, and H. Kleinpoppen, Phys. Rev. Lett. **54**, 1790 (1985).
[12] P. G. Kwiat, A. M. Steinberg, and R. Y. Chiao, Phys. Rev. A **47**, R2472 (1993).

[13] I. A. Khan and J. C. Howell, Phys. Rev. A **73**, 031801(R) (2006).
[14] J. C. Howell, R. S. Bennink, S. J. Bentley, and R. W. Boyd, Phys. Rev. Lett. **92**, 210403 (2004).
[15] J. T. Barreiro, N. K. Langford, N. A. Peters, and P. G. Kwiat, Phys. Rev. Lett. **95**, 260501 (2005).
[16] A. Mair, A. Vaziri, G. Weihs, and A. Zeilinger, Nature **412**, 313 (2001).
[17] A. Vaziri, G. Weihs, and A. Zeilinger, Phys. Rev. Lett. **89**, 240401 (2002).
[18] M. Stütz, S. Gröblacher, T. Jennewein, and A. Zeilinger, Appl. Phys. Lett. **90**, 261114 (2007).
[19] S. Groblacher, T. Jennewein, A. Vaziri, G. Weihs, and A. Zeilinger, New J. Phys. **8**, 75 (2006).
[20] A. Aiello, S. S. R. Oemrawsingh, E. R. Eliel, and J. P. Woerdman, Phys. Rev. A **72**, 052114 (2005).
[21] S. S. R. Oemrawsingh, X. Ma, D. Voigt, A. Aiello, E. R. Eliel, G. W. 't Hooft, and J. P. Woerdman, Phys. Rev. Lett. **95**, 240501 (2005).
[22] J. Leach, B. Jack, J. Romero, M. Ritsch-Marte, R. W. Boyd, A. K. Jha, S. M. Barnett, S. Franke-Arnold, and M. J. Padgett, Opt. Express **17**, 8287 (2009).
[23] E. Yao, S. Franke-Arnold, J. Courtial, M. J. Padgett, and S. M. Barnett, Opt. Express **14**, 13089 (2006).
[24] L. Allen, M. W. Beijersbergen, R. J. C. Spreeuw, and J. P. Woerdman, Phys. Rev. A **45**, 8185 (1992).
[25] G. Molina-Terriza, J. P. Torres, and L. Torner, Phys. Rev. Lett. **88**, 013601 (2001).
[26] A. Vaziri, J. W. Pan, T. Jennewein, G. Weihs, and A. Zeilinger, Phys. Rev. Lett. **91**, 227902 (2003).
[27] M. J. Padgett and J. Courtial, Opt. Lett. **24**, 430 (1999).
[28] J. S. Bell, *Speakable and Unspeakable in Quantum Mechanics* (Cambridge University, Cambridge, England, 2008).
[29] G. Molina-Terriza, J. P. Torres, and L. Torner, Opt. Commun. **228**, 155 (2003).
[30] B. Jack, J. Leach, H. Ritsch, S. M. Barnett, M. J. Padgett, and S. Franke-Arnold, New J. Phys. **11**, 103024 (2009).
[31] J. F. Clauser, M. A. Horne, A. Shimony, and R. A. Holt, Phys. Rev. Lett. **23**, 880 (1969).
[32] J. F. Clauser and M. A. Horne, Phys. Rev. D **10**, 526 (1974).
[33] J. Leach, M. R. Dennis, J. Courtial, and M. J. Padgett, New J. Phys. **7**, 55 (2005).
[34] A. Leggett, Found. Phys. **33**, 1469 (2003).
[35] S. Gröblacher, T. Paterek, R. Kaltenbaek, C. Brukner, M. Zukowski, M. Aspelmeyer, and A. Zeilinger, Nature **446**, 871 (2007).
[36] C. Branciard, N. Brunner, N. Gisin, C. Kurtsiefer, A. Lamas-Linares, A. Ling, and V. Scarani, Nature Phys. **4**, 681 (2008).